Aging and Disease
www.aginganddisease.org
Early access date: January 13, 2026
http://dx.doi.org/10.14336/AD.2025.1243

Original Article

Increased Stability of Tristetraprolin mRNA Supports Bone Health and Decreases Frailty During Aging

Ramkumar Thiyagarajan[1], Lixia Zhang[2], Leticia Andrea Rojas Cortez[2], Kyu Hwan Kwack[3], Victoria Maglaras[2,4], Nanda Kumar Yellapu[5], Yukitomo Arao[6], Kenneth L. Seldeen[1], Perry J. Blackshear[6,7], Bruce R. Troen[1*], Keith L. Kirkwood[2*]

[1]Division of Geriatrics, Department of Internal Medicine and Landon Center on Aging, University of Kansas School of Medicine, Kansas City, KS, and Research Service, Veteran Affairs Kansas City Healthcare System, Kansas City, MO, USA. [2]Department of Oral Biology, School of Dental Medicine, University at Buffalo, Buffalo, NY, USA. [3]Department of Oral Microbiology, College of Dentistry, Kyung Hee University, Seoul, Republic of Korea. [4]Department of Periodontics and Oral Medicine and Department of Cariology, Restorative Sciences, and Endodontics, University of Michigan, Ann Arbor, MI, USA. [5]ICMR-vector Control Research Center, Indira Nagar Medical Complex, Puducherry, India. [6]Molecular and Cellular Biology Laboratory, National Institute of Environmental Health Sciences, Research Triangle Park, NC, USA.[7]Departments of Biochemistry and Medicine, Duke University Medical Center, Durham, NC, USA.

[Received October 2, 2025; Revised December 22, 2025; Accepted December 23, 2025]

ABSTRACT: Age-related chronic low-grade inflammation contributes to both frailty and bone loss. One of the key regulators of inflammatory signaling that declines with age is tristetraprolin (TTP), an RNA-binding protein that promotes degradation of pro-inflammatory transcripts. In this study, we investigated whether stabilizing TTP during aging could reduce frailty and enhance bone health by mitigating inflammation and immune dysfunction. We utilized a knock-in mouse model (TTPΔARE), in which an AU-rich region of the 3′ untranslated region was deleted to stabilize TTP mRNA and increase protein expression. Aged TTPΔARE mice had reduced physical frailty scores, a composite measure based on body weight and physical performance, than age-matched wild-type controls (WT). Since frailty is associated with fracture risk, we examined bone structure. Aged TTPΔARE males exhibited significantly higher bone mineral density and improved bone microarchitecture relative to WT mice. Our prior work showed that aging elevates myeloid-derived suppressor cells (MDSCs), which possess osteoclastogenic potential. The monocytic MDSCs (M-MDSCs) from the bone marrow of aged TTPΔARE formed fewer osteoclasts than those from WT mice. Further, transcriptomic analysis of M-MDSCs revealed downregulation of bone resorption and remodeling pathways, along with upregulation of immune activation genes. In addition, immunophenotyping revealed a healthier, youthful-like immune profile in aged TTPΔARE mice, including increased T-cell reservoirs. These findings signify the critical role of TTP in bone health during aging by regulating osteoimmunological induction of M-MDSCs, which leads to a partial reversal of the age-associated immune senescent phenotype, resulting in increased bone mineral density and improved functional capacity during aging.

Keywords: Aging, tristetraprolin, myeloid-derived suppressor cells, osteoclasts

INTRODUCTION

By 2050, nearly 1 in 4 Americans will be 65 or older, as their numbers are expected to grow from 58 million in 2022 to 82 million, marking a 47% increase and posing significant challenges for healthcare and social support systems [1]. With advancing age, the immune system undergoes dynamic changes characterized by both

***Correspondence should be addressed to:** Dr. Bruce R. Troen, Division of Geriatrics, Department of Internal Medicine and Landon Center on Aging, University of Kansas School of Medicine, Kansas, KS, and Research Service, Veteran Affairs Kansas City Healthcare System, Kansas, MO, USA. Email: btroen@kumc.edu. Dr. Keith L. Kirkwood, School of Dental Medicine, University at Buffalo, Buffalo, New York, USA. Email: klkirk@buffalo.edu.

impairment of adaptive immunity and activation of low-grade chronic inflammation. This chronic activation of inflammation associated with aging has been coined 'inflammaging' [2]. These age-related changes, known as immunosenescence, lead to a decline in immune resilience and an increased susceptibility to age-related chronic inflammatory diseases [3, 4].

Tristetraprolin (TTP; also known as NUP475, GOS24, or TIS11) is an mRNA-binding protein encoded by *Zfp36* that inhibits the production of multiple pro-inflammatory cytokines [5]. TTP's primary role is binding to adenosine-uridine rich elements (AREs) in the 3' untranslated regions (3'-UTRs) by virtue of the tandem CCCH zinc finger within target mRNA transcripts, thus destabilizing and promoting mRNA degradation of targets such as *Tnf*, *Il1β*, and *Il6* [5-9]. In global TTP knockout (TTPKO) mice, our group and others have shown increased cytokine production due to increased cytokine mRNA stability [6, 9]. However, unlike some other key RNA-binding proteins, TTP expression declines with advancing age in humans, particularly in the immune system [10], providing a conceptual framework to address the role of TTP in age-related inflammatory diseases.

As we age, hematopoiesis in the bone marrow is driven towards a myeloid lineage, promoting the accumulation of myeloid-derived suppressor cells (MDSC) [11, 12]. These cells can suppress T cell proliferation and function, and they produce pro-inflammatory cytokines. As a heterogeneous population of immune cells, MDSCs are expanded with aging, influencing immune system function and amplifying the inflammaging process [11]. TTP directly impacts MDSC differentiation and function [13, 14]. Our recent studies demonstrated that young TTP-null mice exhibit increased MDSC populations, with a concomitant reduction in lymphocyte populations, suggesting that TTP is a critical cell-intrinsic factor of age-related adaptation in the immune system and inflammaging [13, 14]. Since the interplay between TTP and MDSCs is crucial in aging, restoring TTP function may help to mitigate age-related immunosenescence and chronic inflammatory diseases.

The age-related expansion of MDSCs and declining TTP levels may lead to increased pro-inflammatory cytokines, such as TNF-α and IL-6 [13]. Monocytic MDSCs (M-MDSCs) are known to differentiate into osteoclasts [15]. We and others have shown that the expansion of MDSCs in aging [15] and young TTPKO mice [13, 14] is associated with increased osteoclast formation in both *in vivo* and *ex vivo* conditions and deteriorating bone microarchitecture. Importantly, we have demonstrated that failure to regulate the expression of cytokines at the post-transcriptional level contributes to inflammatory bone loss [16] and spontaneous bone loss with age in TTPKO mice [16, 17]. Meanwhile, the increased expression of TTP (TTPΔARE) in young (3-month-old) mice did not result in any differences in immune cell phenotype, osteoclast formation, or bone health parameters compared to age-matched wild-type mice [13, 14]. Considering the increasing aging population affected by inflammatory diseases and the declining TTP expression in older individuals, it is critical to study the role of TTP during aging on immune phenotype, MDSC gene expression, bone health, and functional capacity. Poor bone health and decreased physical ability to perform daily activities are indicators of a frail state [18, 19]. The Fried Frailty Index is one of the methods used to assess frailty, which includes components such as weight loss, exhaustion, physical inactivity, slowness, and weakness [20]. In the United States, the prevalence of frailty in the non-nursing home population ages 65 and older is about 15% [21]. Therefore, understanding the mechanisms connecting inflammaging, immune system alterations, bone health, and frailty is essential for developing targeted interventions to improve the quality of life in aging populations. In this study, we aged the TTPΔARE mice (and age-matched wild-type mice) to 22 months and assessed frailty, bone microarchitecture, osteoclastogenesis, immune phenotype, and M-MDSC gene expression profiles.

MATERIALS AND METHODS

Mice

All studies and experimental protocols were approved by and followed the University at Buffalo, Institutional Animal Care and Use Committee guidelines. TTPΔARE mice were generated as described in a previous study [22]. Briefly, 136 bases of an AU-rich region of the TTP (*Zfp36*) mRNA 3′ UTR were deleted in the mouse genome. PCR using primer 1 (P1: 5′-CGTCTCCCCAT CTTCAATCGT-3′) and primer 2 (P2: 5′-CAACCCCC CCCAAAAAATAGA-3′) was routinely done to genotype the offspring. These primers amplified a 780-bp endogenous *Zfp36* WT allele and a 644-bp mutant *Zfp36* knock-in allele (containing mutant exon 2). All experiments were conducted on homozygous knock-in mice (TTPΔARE). The controls used were littermate C57BL/6N mice sourced from intercrossing TTPΔARE/+ heterozygous mice or C57BL/6N WT mice obtained from previous TTPΔARE/+ heterozygous matings. The male and female TTPΔARE mice were obtained from NIEHS (National Institute of Environmental Health Sciences) or inbred in our animal facility. All the mice were maintained under a 12-hour light and 12-hour dark cycle. Mice were provided ad libitum access to chow.

Functional assessments

Physical performance assessments were performed according to protocols we have described previously. Mice were acclimated before the assessments. The same investigator carried out all experiments during daylight hours. All behavioral tests were conducted blinded to genotype.

Grip strength: To assess grip strength in mice, a grip force meter (Columbus Instruments, Columbus, OH) was used. For each trial, the mouse was held by the tail and positioned so that all four limbs contacted the force meter. Then, the tail was pulled until the mouse released its grip. Mice were allowed 10-second rests between trials. The maximum force recorded from the best three of five trials was used for further analysis.

Gait speed: Gait speed analysis was conducted using an apparatus featuring a hallway that was 1 meter long, 8 cm wide, and 12 cm tall, leading into a darkened "safe house" box. The average of the four trials was used for the analysis.

Treadmill endurance: For each trial, the treadmill belt accelerated from 5 to 35 meters per minute over 60 minutes, and the duration on the belt was recorded for each mouse until exhaustion, defined as either 10 visits to a shock pad or 20 total shocks (shocks at 54V, 0.72mA). The data was obtained as the best of two assessments conducted on consecutive days on a mouse treadmill (Columbus Instruments) set to zero incline.

Open-field activity: Mouse activity was assessed using an open-field arena with infrared photobeam arrays (Med Associates Inc., Fairfax, VT). Each arena was 40 cm × 40 cm × 35 cm, and the system software automatically calculated the total distance covered in 30 minutes. After 30 minutes, the total distance traveled, rearings, quadrant crossings, and average speed were calculated by the equipment software (Activity Monitor 7 software, Med Associates Inc).

Frailty assessment: Frailty assessment was performed as described previously [23]. Briefly, the frailty assessment is based on the Fried *et al.* physical frailty assessment for humans [20]. Likewise, this tool for mice includes five parameters, unexpected weight loss (>5% weight loss one week before baseline and before endpoint), and a performance score below a cutoff of 1.5 standard deviations of the baseline group mean comprised of 50% of mice closest to the mean for grip strength, treadmill endurance, gait speed, and open field activity. For this method, mice received 1 point for each parameter below the cut-off point, and mice with three or more such parameters were considered frail (as we have done previously [23, 24]. Briefly, the mean and standard deviation of grip strength, flat continuous treadmill performance, activity monitor crossings, and gait speed were calculated for the WT control mice. The Seldeen50 frailty score was developed to minimize animal variability, which occasionally resulted in one parameter having a cutoff score below zero, rendering it unusable. To address this, the mean and standard deviation were calculated using only the closest 50% of control mice (a total of 6) to the group mean.

FIAV score: The FIAV calculation was performed as described previously [24]. The parameters for FIAV include weight loss, gait speed, grip strength, flat continuous treadmill time on the belt, and activity monitor crossings. To generate a Z-score for each mouse, the value for each parameter is subtracted from the control mean of all mice and then divided by the standard deviation generated from all mice. To reduce variability and address one parameter yielding a negative cutoff score, the Seldeen50 frailty score was calculated using a subset of mice. Specifically, the control mean and standard deviation were derived from the 50% of wild-type mice (n = 6) whose values were closest to the group mean.

Bone microarchitecture

The tibias of TTPΔARE and WT mice were fixed in 10% phosphate-buffered formalin at room temperature for 48 hours, stored in 70% ethanol, and imaged using a high-resolution Scanco Medical 100µCT scanner (Scanco Medical, Bruettisellen, Switzerland) as described in our recent publication [15]. Briefly, mid-shaft and proximal tibias were scanned in an ethanol medium at 70 kVP, 114 µA, a 15.2 mm FOV, 500 projections/180°, 500 ms integration time, and a voxel size of 12 µm. All specimens were scanned under the same conditions. Three-dimensional images were generated, reconstructed, and analyzed using AnalyzePro software (AnalyzeDirect, Inc., Overland Park, KS). These images were rotated to a standard orientation and thresholded to distinguish between mineralized and non-mineralized tissue. Trabecular parameters were obtained from a 960 µm region of interest distal to where the growth plate opened. The 960 µm cortical region of the tibia was derived from 1200 slices distal to the growth plate. All images were analyzed individually, and the ROI was applied. The following trabecular and cortical parameters were calculated using AnalyzePro software: bone volume fraction (BV/TV, %), trabecular thickness (Tb.Th, mm), trabecular separation (Tb.Sp, mm), trabecular number (Tb.N, 1/mm), cortical bone area (Ct.Ar), total cross-sectional area inside the periosteal envelope (Tt.Ar), cortical area fraction (Ct.Ar/Tt.Ar), and average cortical thickness (Ct.Th). All microCT scanning and analyses adhered to bone microstructure guidelines for rodents published by the American Society for Bone and Mineral Research (ASBMR) [25].

Flow cytometry

The single-cell suspensions obtained from bone marrow, spleen, and mesenteric lymph nodes were blocked using mouse BD Fc block (BD Biosciences). The cells were then immunophenotyped with various anti-mouse antibodies [15] listed with catalog numbers in Supplementary Table 1. After staining, the cells were washed and fixed in 1% paraformaldehyde (Sigma Aldrich, St. Louis, MO). Samples were analyzed on an LSR II flow cytometer (BD Biosciences) using FACSDiva version 6.1.3 software. Data analysis was conducted with FlowJo plugins (FlowJo LLC).

M-MDSCs isolation

Bone marrow monocytic myeloid-derived suppressor cells (M-MDSCs) were magnetic sorted from TTPΔARE and WT mice. The mouse myeloid-derived suppressor cell isolation kit (Miltenyi Biotec, Germany) and Miltenyi autoMACS pro were used to sort M-MDSCs following the manufacturer's protocol. Briefly, M-MDSCs were enriched by depleting non-myeloid cells or Gr-1^{high}Ly-$6G^{+}$ cells using a lineage depletion cocktail, followed by positive selection of $Ly6C^{+}$ cells. The purity of the isolated M-MDSCs was assessed by flow cytometry, confirming a population exceeding 85%.

Osteoclastogenesis assay

The M-MDSCs isolated from TTPΔARE (n = 4) and WT (n = 4) mice were seeded at $1x10^5$ cells per well in a 48-well plate for osteoclastogenic differentiation. The M-MDSCs were cultured with monocyte colony-stimulating factor (M-CSF; 25 ng/ml, R&D Systems, BioTechne) and RANKL (50 ng/ml, R&D Systems, BioTechne) in α-MEM media (Gibco, Thermo Fisher Scientific) supplemented with 10% FBS and 1% penicillin/streptomycin. Cells that were stained with tartrate-resistant acid phosphatase (TRAP), and those containing three or more nuclei, were identified as osteoclasts. ImageJ software was utilized to analyze the area of the osteoclasts.

Bulk RNA sequencing

Total RNA was isolated from the magnetically sorted M-MDSCs from TTPΔARE (n = 4) and WT (n = 6) mice using the RNeasy Mini Kit (Qiagen, USA). Whole-genome sequencing was performed using the NovaSeq 6000 System (Illumina Inc., San Diego, CA) at the Genomics and Bioinformatics Core of the New York State Center of Excellence in Bioinformatics and Life Sciences, University at Buffalo, NY as described in our recent publication [15]. FastQC and FastQ were used to review the sequencing quality and detect potential contamination, respectively. Bioconductor package DESeq2 version 1.32.0. was used to detect the differentially expressed genes. Genes with adjusted p-values (padj < 0.05) were considered statistically significant. P-values were adjusted using the Benjamini-Hochberg method to control for false discovery rate (FDR). Genes with log2 fold change > 0 were considered upregulated, and those < 0 were considered downregulated.

Gene ontology enrichment analysis

Significantly upregulated and downregulated genes were used as input for gene ontology (GO) enrichment analysis using the ClusterProfiler package in R. The enrichGO function was used to identify significantly enriched GO terms, with FDR correction applied using the Benjamini-Hochberg method. GO terms were ranked by adjusted p-value and visualized using bubble plots.

Statistical analysis

The graphs were created, and statistical analyses were conducted using GraphPad Prism 10 version 10.4.0 (GraphPad Software Inc., La Jolla, CA). Two-tailed unpaired Student's t-tests and one- or two-way ANOVA followed by GraphPad's recommended post-hoc tests were used as appropriate. All behavioral assessments, histological analyses, and flow cytometry were performed by investigators blinded to genotype and sex. Sample sizes were determined based on previous studies from our group [23, 24], which detected significant differences in frailty scores and FIAV (e.g., $p<0.05$ for HIIT-induced reductions in frailty with n=9–14 per group in aged C57BL/6 mice). Post-hoc power calculations (using G*Power 3.1.9.7) for unpaired two-tailed Student's t-tests confirm that our sample sizes (males: WT n=12, TTPΔARE n=16; females: WT n=12, TTPΔARE n=13) provide >80% power to detect large effect sizes (Cohen's d ≥1.2) at α=0.05 for between-genotype comparisons. Data are shown as mean ± SD; $P < 0.05$ was considered statistically significant.

RESULTS

Increased Stability of TTP (ΔARE) Decreases Frailty in Aged Mice

TTP levels naturally decline with age [10], leading to increased inflammation [7-9], and may contribute to frailty and reduced physical performance. To study the protective effects of stabilized TTP expression during aging, we performed frailty and functional testing in

TTPΔARE mice aged at 22 months. The frailty score, which reflects performance-based physical decline, was significantly lower in aged TTPΔARE male (*n=16*) and female (*n=13*) mice compared to wild-type (WT) controls (*n=12, each sex*) (Fig. 1B), indicating reduced frailty. The mice were classified according to the adapted Fried criteria as robust (score 0), pre-frail (score 1–2), or frail (score ≥ 3). In both sexes, TTPΔARE mice exhibited a striking shift away from frailty.

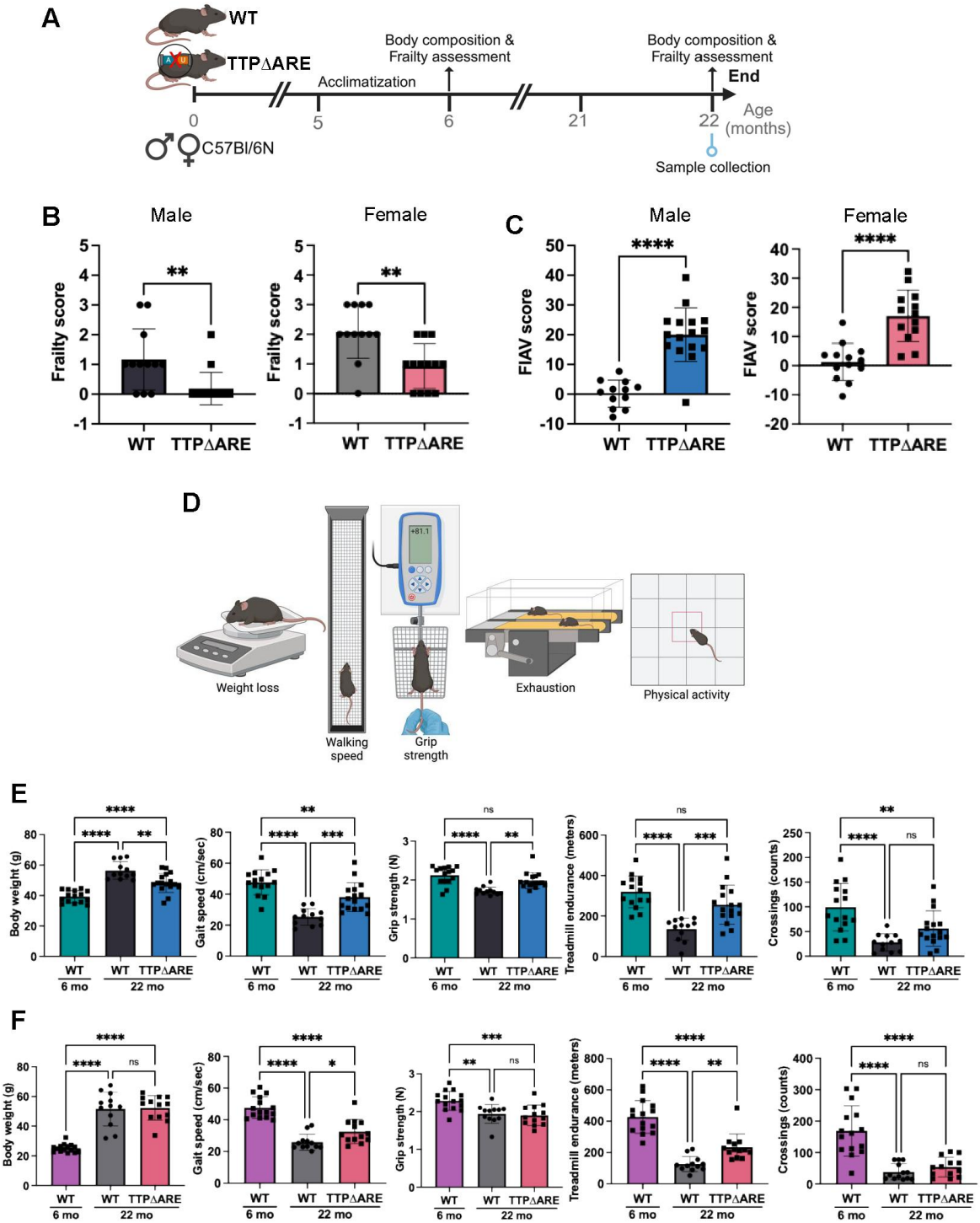

Figure 1. Aged TTPΔARE mice exhibit reduced frailty and improved physical performance. (A) Schematic representation of the study design for evaluating frailty and physical performance in aged mice up to 22 months of age. **(B)** Comparison of Fried Frailty Index between aged male and female TTPΔARE and age- and sex-matched WT mice. Each dot represents a mouse: aged male TTPΔARE (n = 16), aged female TTPΔARE (n = 13), aged male WT (n = 12), and aged female WT (n = 12). **(C)** Frailty

Intervention Assessment Value (FIAV) scores in aged male and female TTPΔARE mice compared to WT mice. **(D)** Schematic diagram depicting the five components used to assess frailty: weight loss, walking speed, grip strength, exhaustion, and physical activity. **(E)** Assessment of frailty components in young (n = 15), aged WT (n = 12), and aged TTPΔARE (n = 16) male mice. **(F)** Comparison of the frailty components in female mice between young (n = 15), aged WT (n = 12), and aged TTPΔARE (n = 13) groups. Statistical differences between the groups were analyzed using a one-way analysis of variance (ANOVA), followed by Tukey's post hoc test for multiple comparisons. Data are presented as mean ± SD, **p<0.01, ***p<0.001, and ****p<0.001.

Among males, no TTPΔARE mice were frail (0/16, 0%) compared to 2/12 (17%) in WT controls, with the majority of TTPΔARE males being robust (14/16, 88%) versus only 3/12 (25%) in WT mice (pre-frail: 2/16 [13%] TTPΔARE vs. 7/12 [58%] WT). Similarly, in females, frailty was completely absent in TTPΔARE mice (0/10, 0%) compared to 4/15 (27%) in WT controls, with TTPΔARE females predominantly pre-frail or robust (pre-frail: 7/10 [70%]; robust: 3/10 [30%]) versus 9/15 (60%) pre-frail and 2/15 (13%) robust in WT females. Thus, at 22 months, TTPΔARE mice of both sexes are predominantly robust or pre-frail compared to age-matched WT mice. In parallel, we also determined the Frailty Intervention Assessment Value (FIAV), which was calculated by converting individual gait speed, grip strength, treadmill endurance, and quadrant crossings into z-scores relative to the group mean and summing them as previously described by our group [24]. We found significantly higher FIAV in both male and female aged TTPΔARE mice (Fig. 1C), indicating a greater functional capacity. A schematic overview of the Fried frailty components is shown in Figure 1D. To assess whether TTPΔARE mice retained youth-like function into old age, we compared physical performance in 22-month-old (aged) TTPΔARE mice to both age-matched WT controls and 6-month-old WT mice. Compared to age-matched WT controls, 22-month-old TTPΔARE males exhibited significantly decreased body weight and increased gait speed, grip strength, and treadmill endurance (Fig. 1E). However, quadrant crossings, a measure of exploratory behavior, were not significantly different in aged TTPΔARE mice (p = 0.127). Notably, grip strength and treadmill endurance of aged TTPΔARE mice were comparable to 6-month-old WT mice. Similarly, aged TTPΔARE females exhibited significantly higher gait speed and treadmill endurance than aged WT females, while grip strength and crossings were not significantly different between aged WT and TTPΔARE females (Fig. 1F). Body weight increased significantly with age in both WT and TTPΔARE mice, but unlike males, no significant difference was observed between aged WT and TTPΔARE females.

TTPΔARE Enhanced Bone Microarchitecture in Aged Mice

As frailty is associated with bone health [26, 27], we next investigated whether reduced frailty observed in aged TTPΔARE mice correlates with improved bone microarchitecture. To assess the impact of the TTPΔARE mutation on bone health, we analyzed the tibia microarchitecture of aged TTPΔARE and WT mice. A schematic representation of the tibia cross-section highlights the regions of interest (ROIs) used for trabecular and cortical analyses (Fig. 2A). Representative micro-computed tomography (micro-CT) images of trabecular and cortical regions indicated structural differences between TTPΔARE male and WT male mice (Fig. 2B). Quantitative analysis further revealed that aged TTPΔARE mice exhibit significantly improved bone parameters, including increased bone mineral density (BMD), bone volume fraction (BV/TV), cortical thickness (Ct.Th), cortical area (Ct. Ar), and cortical area to total area ratio (Ct. Ar/Tt.Ar) compared to WT controls (Fig. 2C). We also evaluated tibial bone microarchitecture in aged TTPΔARE and WT females (Supplementary Fig. 1). Quantitative analysis revealed no significant differences between aged WT and TTPΔARE female mice in trabecular or cortical bone parameters (Supplementary Fig. 1). Further analysis revealed that, aged TTPΔARE males exhibited significantly higher BMD than WT controls (2750.8 ± 264.3 vs. 2504.1 ± 254.8; ~10% increase), along with greater trabecular bone volume fraction (BV/TV; 27.40 ± 3.46% vs. 23.95 ± 2.67%; ~14% increase). In females, BMD values were comparable between genotypes (2806.6 ± 217.8 vs. 2817.5 ± 205.1; ~0.4% difference), while BV/TV showed a modest elevation in TTPΔARE mice (25.70 ± 3.30% vs. 23.78 ± 2.61%; ~8% increase). These results suggest that the skeletal benefits observed in aged TTPΔARE male mice are sex-specific and not evident in females.

TTPΔARE Reduced Osteoclast Formation in Aged Bone Marrow M-MDSCs

Following our observation that aged TTPΔARE mice showed enhanced bone microarchitecture, we studied the cellular mechanisms involved by analyzing the tartrate-resistant acid phosphatase (TRAP) positive cells in the tibia and the osteoclastogenic potential of bone marrow (BM) cells. There were significantly fewer TRAP-positive osteoclasts in trabecular and cortical regions in aged TTPΔARE mice compared to WT mice (Fig. 3A). This reduction in TRAP-positive osteoclasts was confirmed by quantification, with representative cells indicated by arrows in Figure 3A. The number of

osteoclasts per bone perimeter (N.Oc/B.Pm, /mm) and osteoclast surface per bone surface (Oc.S/BS, %) were significantly reduced in TTPΔARE mice (Fig. 3B).

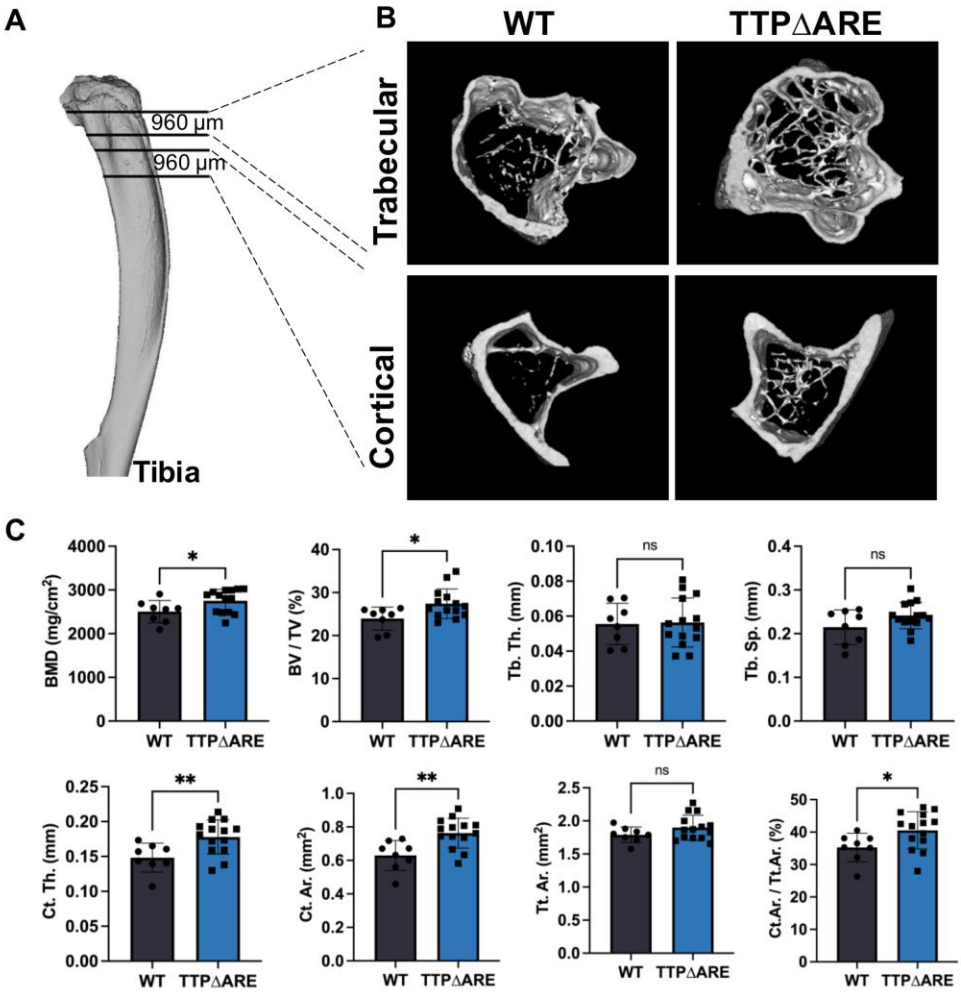

Figure 2. Aged TTPΔARE mice exhibit improved bone microarchitecture compared to WT mice. (A) Schematic representation of the tibia cross-section showing the regions of interest (ROI) for assessing trabecular and cortical bone parameters. **(B)** Representative trabecular and cortical microCT images of tibiae from WT (n = 8) and TTPΔARE (n = 14) male mice. **(C)** Quantitative analysis showing increased bone mineral density (BMD), bone volume to total volume (BV/TV), cortical thickness (Ct.Th), cortical area (Ct.Ar), and cortical area to total area ratio (Ct.Ar/Tt.Ar) in aged TTPΔARE mice compared to WT mice. Statistical significance was determined using unpaired two-tailed Student's t-test. Data represent males only; female data shown in Supp. Fig. 1. Data are presented as mean ± SD, *p<0.05, **p<0.01.

To explore the source of these differences, we isolated one class of osteoclast precursor cells that expand with aging, monocytic myeloid-derived suppressor cells (M-MDSCs) from BM and differentiated them into osteoclasts *ex vivo* using receptor activator of nuclear factor kappa-B ligand (RANKL) and macrophage colony-stimulating factor (M-CSF). M-MDSCs from aged TTPΔARE mice formed fewer osteoclasts than WT mice (Fig. 3C). Quantitative analysis showed fewer osteoclasts ($p<0.001$) and smaller osteoclast areas ($p<0.0001$) in aged TTPΔARE mice (Fig. 3D). To determine whether similar cellular mechanisms underlie the skeletal phenotype in females, we examined bone histology and osteoclast activity in aged WT and TTPΔARE female mice (Supplementary Fig. 2). TRAP staining revealed significantly fewer osteoclasts per field and reduced osteoclast area in tibial sections from aged TTPΔARE females compared to WT controls (Supplementary Fig. 2A and 2B). Further, M-MDSCs isolated from the BM of aged TTPΔARE female mice made fewer osteoclasts than

WT mice (Supplementary Fig. 2C). Quantitative analysis showed significantly fewer osteoclast numbers and smaller osteoclast areas ($p<0.0001$) in aged TTPΔARE mice compared to WT mice (Supplementary Fig. 2D). Similarly, in young TTPΔARE mice, there were significantly reduced osteoclast numbers in the tibia and diminished osteoclastogenic potential of bone marrow–derived M-MDSCs (Supplementary Fig. 7).

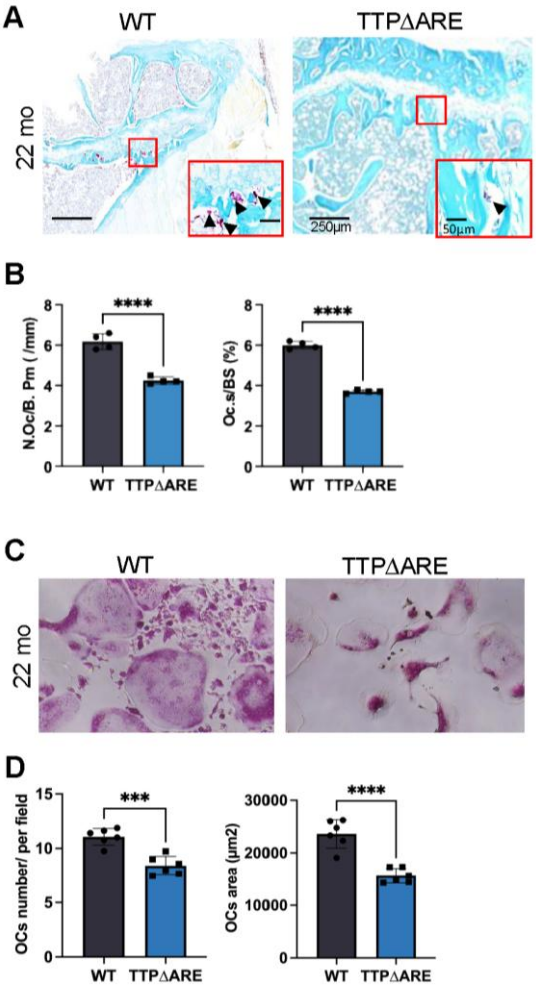

Figure 3. Aged TTPΔARE mice exhibit reduced osteoclasts in tibia and diminished osteoclastogenic potential of bone marrow-derived M-MDSCs. (A) Representative tibial TRAP (tartrate-resistant acid phosphatase) staining showing TRAP-positive osteoclasts in aged WT (n = 4) and TTPΔARE (n = 4) male mice. **(B)** Quantification of osteoclast parameters, including osteoclast numbers per bone perimeter (N.Oc/B.Pm, /mm) and osteoclast surface per bone surface (OC.S/BS, %). **(C)** Ex vivo differentiation of M-MDSCs (monocytic myeloid-derived suppressor cells) into osteoclasts using RANKL (receptor activator of NF-κB ligand) and M-CSF (macrophage colony-stimulating factor). **(D)** Quantification of osteoclast numbers and osteoclast surface area following ex vivo osteoclastogenesis in WT (n = 6) and TTPΔARE (n = 6) male mice. Statistical significance was determined using an unpaired two-tailed Student's t-test. Data represent males only; female data shown in Supp. Fig. 2. Data are presented as mean ± SD; *p<0.05, **p<0.01, ***p<0.001. Scale bars: 250 µm (full-section images), 50 µm (enlarged insets).

Effect of TTPΔARE on Bone Marrow Immune Cell Populations

We next investigated whether reduced osteoclastogenic potential in bone marrow M-MDSCs was accompanied by alterations in the overall immune cell profiles critical to aging and immunosenescence. Bone marrow cells were isolated and immunophenotyped using flow cytometry, with a gating strategy designed to identify M-MDSC and PMN-MDSC populations (Fig. 4A). Uniform Manifold Approximation and Projection (UMAP) analysis visualized the distribution of M-MDSCs, polymorphonuclear myeloid-derived suppressor cells (PMN-MDSCs), and macrophages, with bar graphs illustrating the percentage of each cell type (Fig. 4B and 4C). Aged TTPΔARE male mice displayed a significant decrease in PMN-MDSCs and no difference in M-MDSCs compared to WT mice (Figure 4C). The T-cell compartments, B-cells, dendritic cells (DCs), and natural killer cells (NKs) were visualized using UMAP projections for T-helper (CD4+), T-cytotoxic (CD8+), T-regulatory (Treg) cells, B cells, DCs, and NK cells (Fig. 4D and 4E), with percentage distributions (Fig. 4F and 4G). Aged male TTPΔARE mice exhibited a significant increase in CD4+ T-helper cells and T-reg cells, but no statistically significant difference in CD8+ T-cytotoxic cells, and a significant decrease in DCs, while B-cell and NK-cell levels remained unchanged. Further, there was a trend ($p = 0.081$) towards decrease in interleukin-17 (IL-17) levels in bone marrow (Fig. 4H) observed in aged TTPΔARE mice compared to WT mice. Similar to the male mice, no significant difference in M-MDSCs, PMN-MDSCs, and

macrophages in the BM of aged female TTPΔARE mice compared to WT controls (Supplementary Fig. 3A). Unlike the aged male TTPΔARE male mice, the CD8+ T-cytotoxic cells significantly increased in aged female TTPΔARE mice, but there were no differences in T-helper and T-reg cells (Supplementary Fig. 3B). Aged TTPΔARE female mice exhibited no significant differences in B-cells, DC, NK cells, and IL-17 cells (Supplementary Fig. 3C and 3D).

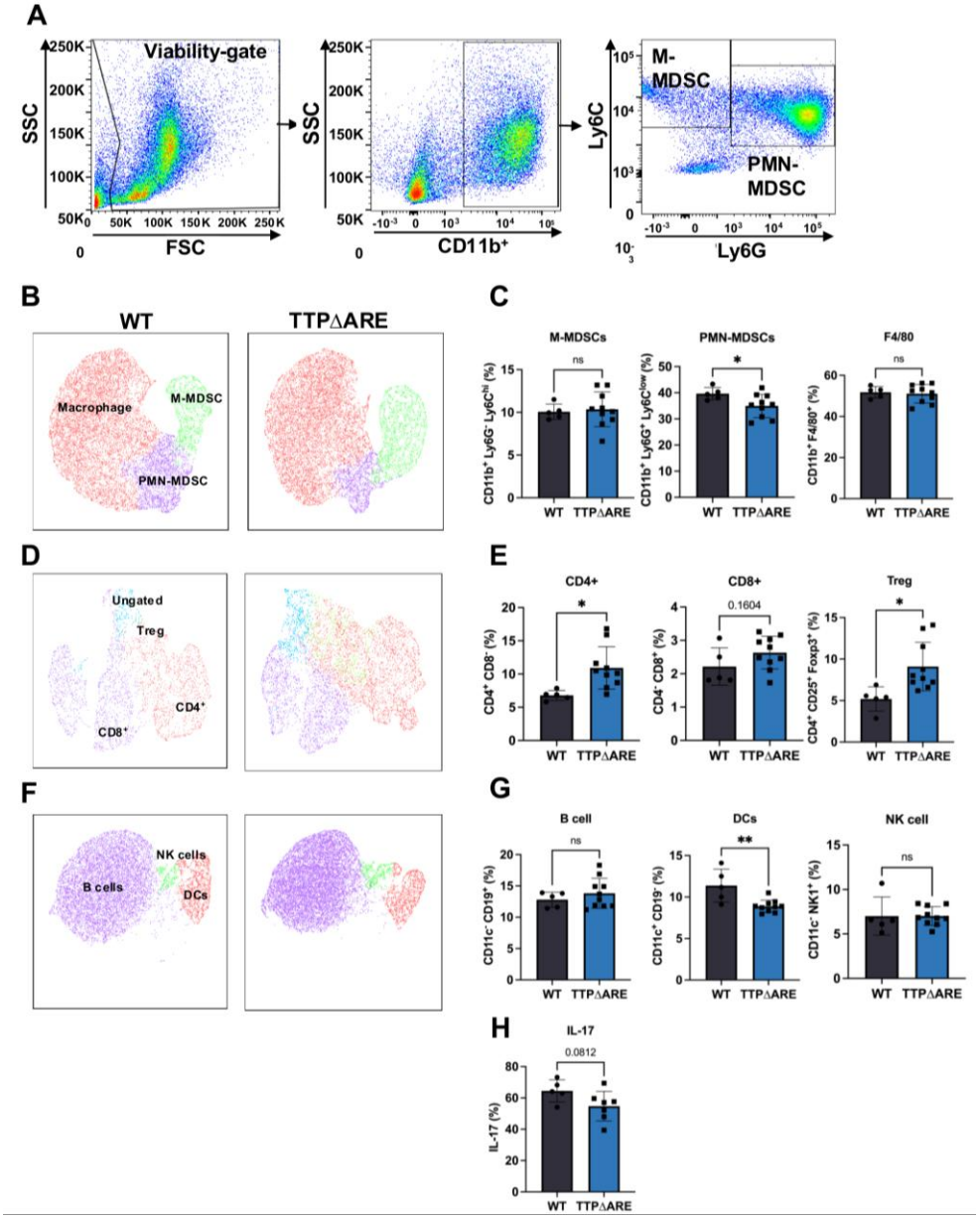

Figure 4. Aged TTPΔARE mice exhibit a healthier immunophenotype with increased T-cell reservoirs. (A) Flow cytometric gating strategy for identifying immune cell populations, including monocytic myeloid-derived suppressor cells (M-MDSCs) and polymorphonuclear myeloid-derived suppressor cells (PMN-MDSCs). **(B)** UMAP plots illustrating bone marrow myeloid populations, including M-MDSCs, PMN-MDSCs, and macrophages. **(C)** Quantification of identified myeloid populations. **(D)** UMAP plots of lymphoid populations, including T-cytotoxic, T-helper, T-regulatory cells, B cells, dendritic cells, and natural killer cells. **(E)** Quantification of lymphoid populations. **(F)** UMAP plots of B-cells, dendritic cells, and natural killer cells and their quantification **(G)**. Experimental groups: WT (n = 5) and TTPΔARE (n =10) male mice. Statistical significance was determined using an unpaired two-tailed Student's t-test. Data represent males only; female data shown in Supp. Fig. 3. Data are presented as mean ± SD, *p<0.05, **p<0.01.

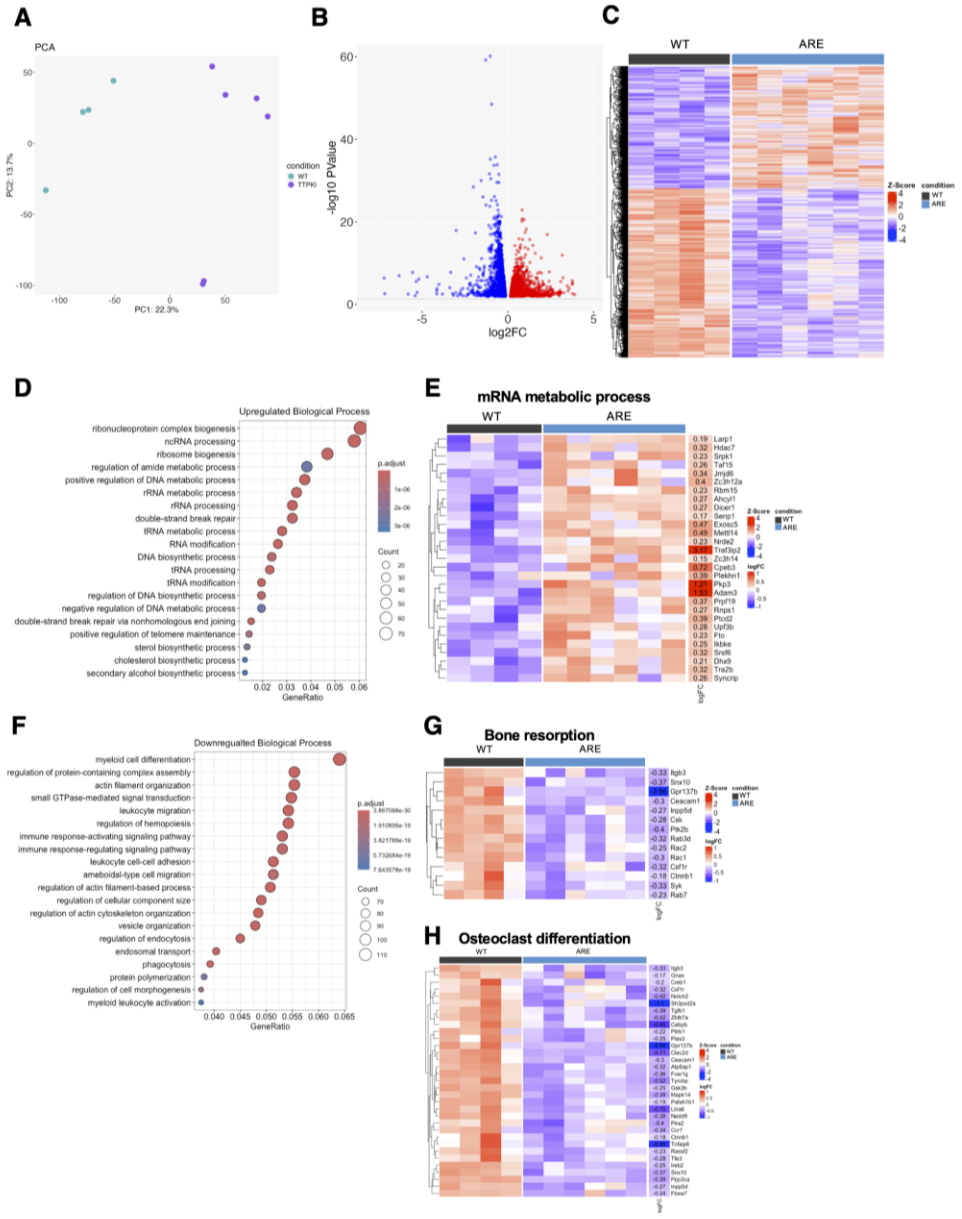

Figure 5. Aged TTPΔARE mice M-MDSCs exhibit distinct gene expression profiles and downregulated bone resorption GO term. (A) PCA plot illustrating the segregation of gene expression profiles between WT and TTPΔARE M-MDSCs. **(B)** Volcano plot depicting significantly upregulated (red) and downregulated (blue) genes in M-MDSCs from male TTPΔARE compared to WT male mice. **(C)** Heatmap showing differentially expressed genes (DEGs) between WT and TTPΔARE groups. **(D)** Gene Ontology (GO) analysis of the top 20 upregulated biological processes. **(E)** GO analysis highlighting enrichment of mRNA metabolic processes. **(F)** GO analysis of downregulated biological processes. Downregulation of bone resorption **(G)** and osteoclast differentiation **(H)** pathways in TTPΔARE M-MDSCs. Experimental groups: WT (n = 4) and TTPΔARE (n = 6) male mice. Female data shown in Supplementary Figure 4.

In the spleen and mesenteric lymph nodes (mLNs), aged male TTPΔARE mice exhibited no statistically significant differences in M-MDSCs, PMN-MDSCs, and macrophages compared to WT mice (Supplementary Fig. 6A and 6B). Surprisingly, the M-MDSCs were significantly reduced in the spleen and mLN of aged TTPΔARE female mice (Supplementary Fig. 3A). $CD4^+$ and $CD8^+$ T-cells were significantly increased in the spleen and mLN of both TTPΔARE female (Supplementary Fig. 3B) and male (Supplementary Fig.

6A) mice. Whereas T-regs were only increased ($p<0.05$) in the mLN, but not in the spleen, of both sexes. B-cell frequencies were significantly decreased in both spleen and mLNs of aged TTPΔARE females (Supplementary Fig. 3C), but a similar change in B-cells was observed only in mLN of TTPΔARE males (Supplementary Fig. 6B). Dendritic cells were significantly decreased in the mLNs of males and showed no reduction in TTPΔARE females. NK cells were significantly reduced in the spleen of males but unchanged in females. IL-17–producing cells were significantly increased in the spleen of both males (Supplementary Fig. 6B) and females (Supplementary Fig. 3D), with unchanged in BM and mLNs. In young (6-month-old) male mice, the TTPΔARE genotype exhibited minimal overall differences in myeloid and lymphoid immune cell populations across BM, SPL, and MLN compared to WT controls, though a significant reduction in PMN-MDSCs was observed in BM and significant elevations in M-MDSCs in spleen and CD8+ cells in SPL (Supplementary Fig. 8A-B). B cells, dendritic cells, and NK cells remained largely comparable between genotypes, with no notable changes in all tissues (Supplementary Fig. 8C). IL-17-producing T cells were significantly higher in TTPΔARE spleen but similar elsewhere (Supplementary Fig. 8D). In contrast, in young female mice, immune profiles showed no major genotype-specific alterations, with only statistically significant increase in CD8+ cells in MLN (Supplementary Fig. 9A-D).

Effect of TTPΔARE on M-MDSC Gene Expression

Aging is marked by a decline in T-cell populations, a key factor driving immunosenescence [28]. M-MDSCs play a pivotal role in modulating T-cell populations through their suppressive functions. Previous studies, including ours, have shown that M-MDSCs possess high osteoclastogenic potential, even though their proportions in bone marrow remain unchanged between young and old mice or young WT and TTPΔARE mice [14, 15]. Despite these similarities, M-MDSCs from aged male TTPΔARE mice exhibit distinct gene expression profiles compared to WT mice. Principal component analysis (PCA, Fig. 5A) demonstrated a clear separation between aged WT and TTPΔARE M-MDSCs. Differential expression analysis identified significant upregulation and downregulation of genes, visualized in a volcano plot (Fig. 5B). Heatmaps (Fig. 5C) further showcased a distinct transcriptional landscape in TTPΔARE M-MDSCs. In addition, gene ontology (GO) analysis revealed upregulation of pathways associated with mRNA metabolism (Fig. 5E) and mitochondrial gene expression (Fig. 5F), while pathways linked to bone resorption (Fig. 5G) and osteoclast differentiation (Fig. 5H) were downregulated. Interestingly, we observed a similar pattern of transcriptomic remodeling in M-MDSCs isolated from aged female TTPΔARE mice (Supplementary Fig. 4A-H). Principal component analysis and differential gene expression revealed distinct clustering and separation from aged WT controls. Gene ontology analysis showed upregulation of pathways involved in mRNA metabolism and mitochondrial function, while pathways related to bone resorption and osteoclast differentiation were downregulated, mirroring the changes observed in male TTPΔARE M-MDSCs. These data suggest that stabilized TTP expression alters key inflammatory and osteogenic gene programs in M-MDSCs of both sexes during aging.

DISCUSSION

Enhancing TTP expression throughout the lifespan of male and female mice improved frailty scores, reflecting improvements in body weight, gait speed, grip strength, and physical activity. Both male and female aged TTPΔARE mice exhibited significantly reduced frailty scores and increased FIAV scores compared to WT controls during aging. The significant reductions in Fried Frailty Score and improvements in FIAV observed at 22 months prior to the rapid acceleration phase of frailty in C57BL/6 mice, with onset around 17 months at low prevalence, gradual progression until approximately 23 months, and steep increase thereafter [29], indicate that the constitutive global TTP stabilization model used in this study primarily exerts preventive effects, attenuating the accumulation of age-related functional deficits during the early-to-mid phase of frailty development. Notably, grip strength and treadmill endurance in aged TTPΔARE male mice, but not in aged TTPΔARE female mice, were restored to levels comparable to those of young (6-month-old) WT mice, suggesting that enhanced TTP expression reverses specific aspects of age-related physical decline. This partial preservation of youth-like function implies that TTP stabilization can attenuate or delay the functional impairments typically associated with aging. However, the extent of protection differed, with aged males showing restoration across all individual FIAV components, including body weight, grip strength, and gait speed, whereas aged females exhibited significant improvements only in select measures such as gait speed and treadmill endurance. Overall, these results suggest that TTP stabilization confers less robust protection in females. Similar sex differences in frailty appear across various preclinical models [30]. These differences likely arise from behavioral, social, and biological factors, significantly impacting disease susceptibility, treatments, and outcomes in the frail elderly population [30, 31]. This minor sex-specific difference likely reflects the complex

interplay between hormonal environment, immune aging, and post-transcriptional regulation. While TTP modulates inflammatory gene expression in both sexes, estrogen loss during aging may limit its capacity to fully restore musculoskeletal function in females. In this study, the lack of improvement in grip strength and crossings in aged TTPΔARE females, despite preserved gait and endurance, suggests that age-related estrogen decline may restrict tissue responsiveness to anti-inflammatory modulation. This aligns with known roles of estrogen in regulating the skeletomuscular system, cytokine signaling, and neural activation pathways involved in exploratory behavior.

A key limitation of this study is the global nature of the TTPΔARE, which stabilizes TTP mRNA across all tissues and cell types where TTP is endogenously expressed, rather than being restricted to MDSCs or myeloid cells. TTP exhibits broad expression patterns, including in immune cells (e.g., macrophages, T cells, and dendritic cells), epithelial cells (e.g., keratinocytes and colonic epithelium), fibroblasts, muscle cells, and neural tissues, with levels often declining with age, particularly in the immune system, but also varying by tissue context [10, 32]. This widespread expression suggests that the observed improvements in frailty and physical performance may arise not only from reduced inflammaging and MDSC-driven osteoclastogenesis but also from effects in other systems more directly linked to muscle and neuromotor function. For instance, TTP is expressed in skeletal and cardiac muscle, where it regulates inflammation, cell survival (e.g., in response to nicotinic stimulation), and mitochondrial function, potentially contributing to enhanced grip strength, gait speed, and treadmill endurance independent of systemic inflammation [32]. Similarly, in the nervous system, TTP modulates brain-derived neurotrophic factor expression, protects dopaminergic neurons, and influences sympathetic nerve activity, which could directly impact neuromotor coordination and exploratory behavior (e.g., quadrant crossings) without relying solely on MDSC or cytokine changes [33]. These multifaceted effects highlight the need for future studies using conditional knock-in models to delineate cell- and tissue-specific contributions of TTP to age-related phenotypes, thereby clarifying the relative roles of immune versus non-immune mechanisms in frailty and bone health.

The skeletal benefits of TTP stabilization also appeared to be male-specific, as aged TTPΔARE males demonstrated increased trabecular and cortical bone parameters, while no significant improvement was observed in females. This disparity may result from sexually dimorphic baseline bone architecture or differential osteoclast responsiveness to inflammatory signals. In both clinical and preclinical models, females typically have lower BMD and altered bone microarchitecture compared to males [34, 35]. These changes result in less dense bones with a different bone microarchitecture, increasing their susceptibility to fractures, especially after menopause when estrogen levels decline [36]. Nonetheless, increased TTP expression in both sexes reduced the number of osteoclasts per bone perimeter and osteoclast surface per bone surface in vivo, indicating that TTP limits osteoclastogenesis independent of sex. The limited benefits in females may stem from interactions between TTP and estrogen signaling, as estrogen receptors (ERs) in osteoclasts and osteoblasts mediate protective effects against bone loss by repressing pro-osteoclastic cytokines (e.g., TNF-α, IL-1, and IL-6) and promoting osteoclast apoptosis via Fas/FasL pathways, potentially synergizing with or modulating TTP's anti-inflammatory actions on cytokine mRNA stability [36, 37]. For example, estrogen deficiency elevates these cytokines and RANKL expression, enhancing osteoclastogenesis, a process that could overwhelm TTP-mediated post-transcriptional repression in postmenopausal states [37]. This may explain the lack of bone microarchitecture improvements in aged TTPΔARE females despite reduced osteoclast formation, as estrogen decline attenuates the intersection between hormonal and inflammatory regulatory pathways. Future studies incorporating estrogen measurements, cytokine profiling, ovariectomy models, or ER knockout models could elucidate these sex-specific interactions. Importantly, our previous work demonstrated that the M-MDSCs, which serve as precursors of osteoclasts, expand in various tissues during aging and inflammatory conditions [11, 13]. Furthermore, we revealed the role of TTP in regulating the egress of MDSCs from the BM via the CCR2-CCL2 axis, thereby altering the osteoclastogenic potential of M-MDSCs and driving age-related skeletal deterioration [13, 14]. Here, we further confirm the role of TTP on the osteoclastogenic potential of M-MDSCs, as the M-MDSCs from aged TTPΔARE mice formed fewer and smaller osteoclasts *ex vivo*. Furthermore, the TTP's role in the osteoclastogenic potential of M-MDSCs is independent of sex in aged mice. These *in vitro* changes likely precede the functional skeletal improvements.

Although our findings emphasize reduced osteoclastogenesis as a key mechanism for improved bone health in TTPΔARE mice, a limitation is that we did not directly assess bone formation rates or osteoblast function, which could also contribute to the observed skeletal benefits. TTP (ZFP36) is expressed in osteoblasts, mesenchymal stem cells (MSCs), endothelial cells, and skeletal muscle, where it regulates mRNA stability of genes involved in differentiation, inflammation, and tissue remodeling [38-40]. For instance, ZFP36 promotes osteogenic differentiation in

human bone marrow-derived MSCs by inhibiting the translation of JUN mRNA, potentially enhancing osteoblast activity and bone health [39]. Similarly, in endothelial cells, ZFP36 reduces inflammation in atherosclerotic lesions, which could indirectly support vascularized bone repair during aging [40]. Age-related declines in these cell types may thus be ameliorated by TTP stabilization, contributing to the male-specific improvements in bone microarchitecture beyond MDSC-driven resorption. Future studies incorporating dynamic histomorphometry, osteogenic markers, or conditional models will be essential to explore these contributions.

In addition to their osteoclastogenic potential, M-MDSCs also exert immunosuppressive effects by suppressing T-cell populations, a hallmark of immunosenescence [41, 42]. Therefore, we profiled immune cell populations in the bone marrow, spleen, and mesenteric lymph node (mLN) of aged TTPΔARE and WT mice. In the bone marrow, aged male TTPΔARE mice exhibited a significant reduction in PMN-MDSCs without changes in M-MDSC frequencies, along with increased T-helper and regulatory T-cells, but no significant differences in cytotoxic T-cells. These changes were accompanied by a decrease in dendritic cells, while B-cells and NK-cells remained unchanged. Conversely, aged female TTPΔARE mice exhibited a significant increase in cytotoxic T cells, but no changes in T-helper or T-regulatory populations. Surprisingly, in peripheral tissues, both sexes exhibited significantly increased helper and cytotoxic T-cells in the spleen and mLNs, while T-regs were elevated specifically in the mLNs. Notably, aged TTPΔARE females had significantly lower M-MDSC frequencies in the spleen and mLNs, which was not observed in males. Furthermore, IL-17 producing cells were elevated in the spleens of both sexes. The spleen-specific increase in IL-17-producing cells in aged TTPΔARE mice, despite the broader anti-inflammatory profile, may reflect a compensatory mechanism promoting tissue repair and immune balance rather than pathology. IL-17 exhibits a dual role in aging: while often pro-inflammatory and linked to inflammaging, it can support homeostatic responses, such as neutrophil recruitment for pathogen clearance and resolution or epithelial barrier integrity against microbial translocation, particularly amid age-related T cell shifts in peripheral and secondary lymphoid organs like the spleen [43, 44]. This targeted elevation could thus contribute to the enhanced T cell reservoirs and immune resilience observed, aligning with models where IL-17 restrains excessive inflammaging without driving bone resorption. These findings demonstrate that TTP stabilization supports maintenance of key T-cell subsets and restrains immunosuppressive MDSC populations in a tissue- and sex-specific manner, consistent with a partial reversal of immunosenescence in aged mice.

However, to elucidate the mechanism or pathway by which TTP reduces the osteoclastogenic potential of M-MDSCs, we performed RNA sequencing on M-MDSCs from both males and females. TTPΔARE mice revealed key transcriptional changes, including upregulated RNA metabolism pathways and downregulated osteoclast differentiation pathways. Notably, several genes central to osteoclastogenesis and MDSC inflammatory function such as, *Mapk14* (p38 MAPK), *Tnfaip6*, *Cebpb*, and *Irf1,* were significantly reduced in TTPΔARE M-MDSCs. These genes are known to promote osteoclast differentiation, cytokine signaling, and myeloid-driven immune suppression. In addition, stable expression of TTP reprograms MDSCs by downregulating genes involved in the production of myeloid leukocyte cytokines in males and females (Supplementary Fig. 5). Their suppression reinforces a molecular mechanism by which TTP restrains the osteoclastogenic and pro-inflammatory potential of MDSCs. This transcriptomic remodeling of M-MDSCs supports a systemic mechanism by which TTP reduces inflammaging and age-associated bone loss, even when skeletal outcomes differ between sexes. These shifts explain the reduced osteoclast activity and bone resorption observed in TTPΔARE mice. Collectively, enhanced stability of TTP appears to mitigate age-related immunosenescence and osteoclastogenic potential of M-MDSCs, highlighting TTP as a potential therapeutic target to boost immune resilience and maintain bone health.

This study demonstrates the critical role of TTP in regulating aging processes by reducing frailty, preserving bone integrity, enhancing immune resilience, and altering the transcriptomic profile of M-MDSCs. While the global TTPΔARE knock-in model is not directly translatable to humans, future therapeutic strategies could involve pharmacologic modulation of TTP expression, such as small-molecule gene inducers or mRNA stabilizers, or modulators of RNA-binding and destabilizing activity, such as phosphorylation modifiers. These and other approaches to enhancing TTP activity on pro-inflammatory mRNAs have been reviewed recently [8, 45]. In conclusion, TTPΔARE mice show significant improvements in frailty, bone health, and immune function with age compared to WT mice. Their increased bone mass, reduced osteoclastogenesis, and reprogrammed M-MDSC transcriptional profiles illustrate the role of TTP in regulating inflammation and immune function. These findings position TTP as a promising target for addressing frailty and inflammation associated with aging, paving the way for broader therapeutic exploration. Beyond bone and frailty, TTP modulates neuroinflammation [46], inflammation in

muscle [32], and cardiovascular aging [47], positioning it as a versatile target for multifaceted aging pathologies.

Acknowledgements

This work was supported by the National Institutes of Health (NIH) grants, R01DE028258 (KK), K18DE 029526 (KK), K07AG060266 (BT), K12DE 027826 (VM), BX004369 (BT), and the Indian Trail Foundation (BT) and by the Intramural Research Program of the National Institutes of Health (NIH). The contributions of the NIH author(s) were made as part of their official duties as NIH federal employees, are in compliance with agency policy requirements, and are considered Works of the United States Government. However, the findings and conclusions presented in this paper are those of the author(s) and do not necessarily reflect the views of the NIH or the U.S. Department of Health and Human Services. (PJB and YA). Part of the KHK effort was supported by the Korea Basic Science Institute for National Research Facilities and Equipment Center, with the grant number RS-2024-00404660. Micro-computed tomography and flow cytometry data in this study were acquired at the Optical Imaging and Analysis Facility, School of Dental Medicine, State University of New York at Buffalo.

Author Contributions

Keith Kirkwood conceived and designed all the experiments and edited the manuscript. Ramkumar Thiyagarajan designed behavioral tests, performed experiments, and wrote the original manuscript draft. Lixia Zhang maintained the TTP mouse colony, performed experiments, and edited the manuscript. Leticia Andrea Rojas Cortez assisted with osteoclast experiments and/or bone histology analyses. Kyu Hwan Kwack and Victoria Maglaras analyzed the tibia micro-CT data and flow cytometry and edited the manuscript. Nanda Kumar Yellapu analyzed NextGen RNA sequencing data. Yukitomo Arao maintained the TTP mice colony at NIEHS and provided the young TTPΔARE mice. Perry Blackshear created the TTPΔARE mouse model, provided valuable scientific insights, and edited the manuscript. Kenneth Seldeen and Bruce Troen provided valuable scientific insights, designed behavioral experiments, and edited the manuscript. All authors contributed to the article and approved the submitted version.

Conflict of Interest

The authors declare no competing interests.

Supplementary Materials

The Supplementary data can be found online at: www.aginganddisease.org/EN/10.14336/AD.2025.1243.

References

[1] Bureau. USC (2023). 2023 National Population Projections Tables: Main Series.

[2] Franceschi C, Bonafe M (2003). Centenarians as a model for healthy aging. Biochem Soc Trans, 31:457-461.

[3] Franceschi C, Campisi J (2014). Chronic inflammation (inflammaging) and its potential contribution to age-associated diseases. J Gerontol A Biol Sci Med Sci, 69 Suppl 1:S4-9.

[4] Wrona MV, Ghosh R, Coll K, Chun C, Yousefzadeh MJ (2024). The 3 I's of immunity and aging: immunosenescence, inflammaging, and immune resilience. Front Aging, 5:1490302.

[5] Brooks SA, Blackshear PJ (2013). Tristetraprolin (TTP): interactions with mRNA and proteins, and current thoughts on mechanisms of action. Biochim Biophys Acta, 1829:666-679.

[6] Lai WS, Carballo E, Strum JR, Kennington EA, Phillips RS, Blackshear PJ (1999). Evidence that tristetraprolin binds to AU-rich elements and promotes the deadenylation and destabilization of tumor necrosis factor alpha mRNA. Mol Cell Biol, 19:4311-4323.

[7] Palanisamy V, Jakymiw A, Van Tubergen EA, D'Silva NJ, Kirkwood KL (2012). Control of cytokine mRNA expression by RNA-binding proteins and microRNAs. J Dent Res, 91:651-658.

[8] Patial S, Blackshear PJ (2016). Tristetraprolin as a Therapeutic Target in Inflammatory Disease. Trends Pharmacol Sci, 37:811-821.

[9] Zhao W, Liu M, D'Silva NJ, Kirkwood KL (2011). Tristetraprolin regulates interleukin-6 expression through p38 MAPK-dependent affinity changes with mRNA 3' untranslated region. J Interferon Cytokine Res, 31:629-637.

[10] Masuda K, Marasa B, Martindale JL, Halushka MK, Gorospe M (2009). Tissue- and age-dependent expression of RNA-binding proteins that influence mRNA turnover and translation. Aging (Albany NY), 1:681-698.

[11] Beerman I, Bhattacharya D, Zandi S, Sigvardsson M, Weissman IL, Bryder D, et al. (2010). Functionally distinct hematopoietic stem cells modulate hematopoietic lineage potential during aging by a mechanism of clonal expansion. Proc Natl Acad Sci U S A, 107:5465-5470.

[12] Dorrington MG, Bowdish DM (2013). Immunosenescence and novel vaccination strategies for the elderly. Front Immunol, 4:171.

[13] Kwack KH, Zhang L, Kramer ED, Thiyagarajan R, Lamb NA, Arao Y, et al. (2022). Tristetraprolin limits age-related expansion of myeloid-derived suppressor cells. Front Immunol, 13:1002163.

[14] Zhang L, Kwack KH, Thiyagarajan R, Mullaney KK, Lamb NA, Bard JE, et al. (2024). Tristetraprolin regulates the skeletal phenotype and osteoclastogenic potential through monocytic myeloid-derived suppressor cells. FASEB J, 38:e23338.

[15] Thiyagarajan R, Zhang L, Glover OD, Kwack KH, Ahmed S, Murray E, et al. (2024). Age-related increase of CD38 directs osteoclastogenic potential of monocytic myeloid-derived suppressor cells through mitochondrial dysfunction in male mice. Aging Cell, 23:e14298.

[16] Patil CS, Liu M, Zhao W, Coatney DD, Li F, VanTubergen EA, et al. (2008). Targeting mRNA stability arrests inflammatory bone loss. Mol Ther, 16:1657-1664.

[17] Steinkamp HM, Hathaway-Schrader JD, Chavez MB, Aartun JD, Zhang L, Jensen T, et al. (2018). Tristetraprolin Is Required for Alveolar Bone Homeostasis. J Dent Res, 97:946-953.

[18] Laskou F, Fuggle NR, Patel HP, Jameson K, Cooper C, Dennison E (2022). Associations of osteoporosis and sarcopenia with frailty and multimorbidity among participants of the Hertfordshire Cohort Study. J Cachexia Sarcopenia Muscle, 13:220-229.

[19] Laskou F, Patel H, Cooper C, Dennison E (2022). Functional capacity, sarcopenia, and bone health. Best Pract Res Clin Rheumatol, 36:101756.

[20] Fried LP, Tangen CM, Walston J, Newman AB, Hirsch C, Gottdiener J, et al. (2001). Frailty in older adults: evidence for a phenotype. J Gerontol A Biol Sci Med Sci, 56:M146-156.

[21] Bandeen-Roche K, Seplaki CL, Huang J, Buta B, Kalyani RR, Varadhan R, et al. (2015). Frailty in Older Adults: A Nationally Representative Profile in the United States. J Gerontol A Biol Sci Med Sci, 70:1427-1434.

[22] Patial S, Curtis AD, 2nd, Lai WS, Stumpo DJ, Hill GD, Flake GP, et al. (2016). Enhanced stability of tristetraprolin mRNA protects mice against immune-mediated inflammatory pathologies. Proc Natl Acad Sci U S A, 113:1865-1870.

[23] Seldeen KL, Lasky G, Leiker MM, Pang M, Personius KE, Troen BR (2018). High Intensity Interval Training Improves Physical Performance and Frailty in Aged Mice. J Gerontol A Biol Sci Med Sci, 73:429-437.

[24] Seldeen KL, Redae YZ, Thiyagarajan R, Berman RN, Leiker MM, Troen BR (2019). High intensity interval training improves physical performance in aged female mice: A comparison of mouse frailty assessment tools. Mech Ageing Dev, 180:49-62.

[25] Bouxsein ML, Boyd SK, Christiansen BA, Guldberg RE, Jepsen KJ, Muller R (2010). Guidelines for assessment of bone microstructure in rodents using micro-computed tomography. J Bone Miner Res, 25:1468-1486.

[26] Giannopoulou A (2017). Frailty and bone health in European men. J Frailty Sarcopenia Falls, 2:12-15.

[27] Que Z, Lin Y, Chen D, Xiao K, Xu W, Sun N, et al. (2024). The association between osteoporosis and frailty: a cross-sectional observational study and mendelian randomization analysis. J Orthop Surg Res, 19:398.

[28] Nikolich-Zugich J (2008). Ageing and life-long maintenance of T-cell subsets in the face of latent persistent infections. Nat Rev Immunol, 8:512-522.

[29] Baumann CW, Kwak D, Thompson LV (2018). Assessing onset, prevalence and survival in mice using a frailty phenotype. Aging (Albany NY), 10:4042-4053.

[30] Kane AE, Howlett SE (2021). Sex differences in frailty: Comparisons between humans and preclinical models. Mech Ageing Dev, 198:111546.

[31] Park C, Ko FC (2021). The Science of Frailty: Sex Differences. Clin Geriatr Med, 37:625-638.

[32] Geyer BC, Ben Ari S, Barbash S, Kilbourne J, Mor TS, Soreq H (2012). Nicotinic stimulation induces Tristetraprolin over-production and attenuates inflammation in muscle. Biochim Biophys Acta, 1823:368-378.

[33] Asadi MR, Talebi M, Gharesouran J, Sabaie H, Jalaiei A, Arsang-Jang S, et al. (2022). Analysis of ROQUIN, Tristetraprolin (TTP), and BDNF/miR-16/TTP regulatory axis in late onset Alzheimer's disease. Front Aging Neurosci, 14:933019.

[34] Gabel L, Macdonald HM, McKay HA (2017). Sex Differences and Growth-Related Adaptations in Bone Microarchitecture, Geometry, Density, and Strength From Childhood to Early Adulthood: A Mixed Longitudinal HR-pQCT Study. J Bone Miner Res, 32:250-263.

[35] Ortona E, Pagano MT, Capossela L, Malorni W (2023). The Role of Sex Differences in Bone Health and Healing. Biology (Basel), 12.

[36] Zhang YY, Xie N, Sun XD, Nice EC, Liou YC, Huang C, et al. (2024). Author Correction: Insights and implications of sexual dimorphism in osteoporosis. Bone Res, 12:25.

[37] Hsu SH, Chen LR, Chen KH (2024). Primary Osteoporosis Induced by Androgen and Estrogen Deficiency: The Molecular and Cellular Perspective on Pathophysiological Mechanisms and Treatments. Int J Mol Sci, 25.

[38] Shi DL, Grifone R (2021). RNA-Binding Proteins in the Post-transcriptional Control of Skeletal Muscle Development, Regeneration and Disease. Front Cell Dev Biol, 9:738978.

[39] Su H, Liang L, Wang J, Yuan X, Zhao B (2024). ZFP36, an RNA-binding protein promotes hBMSCs osteogenic differentiation via binding with JUN. J Orthop Surg Res, 19:758.

[40] Zhang H, Taylor WR, Joseph G, Caracciolo V, Gonzales DM, Sidell N, et al. (2013). mRNA-binding protein ZFP36 is expressed in atherosclerotic lesions and reduces inflammation in aortic endothelial cells. Arterioscler Thromb Vasc Biol, 33:1212-1220.

[41] Goronzy JJ, Weyand CM (2003). Aging, autoimmunity and arthritis: T-cell senescence and contraction of T-cell repertoire diversity - catalysts of autoimmunity and chronic inflammation. Arthritis Res Ther, 5:225-234.

[42] Salminen A, Kaarniranta K, Kauppinen A (2019). Immunosenescence: the potential role of myeloid-derived suppressor cells (MDSC) in age-related immune deficiency. Cell Mol Life Sci, 76:1901-1918.

[43] Merino KM, Jazwinski SM, Rout N (2021). Th17-type immunity and inflammation of aging. Aging (Albany NY), 13:13378-13379.
[44] Mills KHG (2023). IL-17 and IL-17-producing cells in protection versus pathology. Nat Rev Immunol, 23:38-54.
[45] Snyder BL, Blackshear PJ (2022). Clinical implications of tristetraprolin (TTP) modulation in the treatment of inflammatory diseases. Pharmacol Ther, 239:108198.
[46] Sun X, Zhang H, Xie L, Qian C, Ye Y, Mao H, et al. (2020). Tristetraprolin destabilizes NOX2 mRNA and protects dopaminergic neurons from oxidative damage in Parkinson's disease. FASEB J, 34:15047-15061.
[47] Ghosh S, Hoenerhoff MJ, Clayton N, Myers P, Stumpo DJ, Maronpot RR, et al. (2010). Left-sided cardiac valvulitis in tristetraprolin-deficient mice: the role of tumor necrosis factor alpha. Am J Pathol, 176:1484-1493.